

Mixing," *Can. J. Chem. Eng.*, **47**, 258 (1969).  
 Specchia, V., and G. Baldi, "Pressure Drop and Liquid Holdup for Two-Phase Cocurrent Flow in Packed Beds," *Chem. Eng. Sci.*, **32**, 515 (1977).  
 Turpin, J. L., and R. L. Huntington, "Prediction of Pressure Drop for Two-Phase, Two-Component Cocurrent Flow in Packed Beds," *AIChE J.*, **13**, 6, 1196 (1976).  
 White, E. T., "Evaluation of the Zakian Numerical Method for Inverting

Laplace Transforms," Automation 77 Conf., Auckland, New Zealand (1977).

Van Swaaij, W. P. M., J. C. Charpentier, and J. Villermaux, "Residence time Distribution in the Liquid Phase of Trickle Flow in Packed Columns," *Chem. Eng. Sci.*, **24**, 1083 (1969).

Manuscript received August 13, 1981; revision received February 23, and accepted March 4, 1982.

# Tortuosity Factors for Diffusion in Catalyst Pellets

The dynamic pulse-response technique was used to measure effective diffusivities under nonreacting conditions in two, unsulfided, extrudate-type, hydro-desulfurization catalyst pellets of different porosities. Pore-volume distribution data showed a bidisperse pore structure with a broad pore-size range (100  $\mu\text{m}$  to 3 nm).

The main purpose of the study was to evaluate various methods for calculating the tortuosity factor,  $\tau$ . For this particular catalyst, the most constant and unreasonable values of  $\tau$  were obtained by supposing that diffusion occurred in all the pore volume (micro and macropores) and by summing the combined Knudsen and bulk contributions over each increment of pore volume.

CHANG-TAI WANG

and

J. M. SMITH

University of California  
 Davis, CA 95616

## SCOPE

Tortuosity factors  $\tau$  are a helpful measure of the effects of pore structure on diffusion in catalyst pellets. When pore sizes are small enough for Knudsen diffusion to be significant and when the distribution of pore volume is over a wide range of pore radii, there is uncertainty in how to evaluate  $\tau$ . When the catalyst pellet is prepared by compressing porous particles, as, for example, for alumina pellets, it has often been assumed that diffusion occurs only in the macropores surrounding the microporous particles. However, it seems more logical to include diffusion in both micro and macropores. Especially when some interparticle pores are smaller than the largest intraparticle pores (micropores), it is preferable to include the total pore volume in evaluating the tortuosity factor. With respect to

Knudsen diffusion, there is the question of the proper pore radius to employ.

The purpose of this paper is to test various methods of evaluating  $\tau$ , including a new approach based upon summing the combined bulk plus Knudsen contributions over the total pore volume. To evaluate the methods, diffusion data are obtained from 298 to 502 K and at 1 atm for pellets of two densities prepared from an extrudate type of unsulfided hydro-desulfurization catalyst. Measurements were made by the dynamic technique (Dogu and Smith, 1975) for He-N<sub>2</sub> and H<sub>2</sub>-N<sub>2</sub> systems, both of which were nonadsorbing. Pore-volume distribution data were also obtained for the two pellets.

## CONCLUSIONS AND SIGNIFICANCE

Both pellets exhibited a wide range of pore diameters from greater than  $10 \times 10^{-5}\text{m}$  to  $3 \times 10^{-9}\text{m}$ . The distribution was bidisperse with nearly the same micropore ( $r < 50 \times 10^{-10}\text{m}$ ) distribution (Figures 1 and 2). The chief difference in pore volume was due to elimination of much of the macropore region for the more dense pellet.

As expected, effective diffusivities were substantially less for the more dense pellet even though the porosity was not much less (0.569) than that (0.677) for the less dense pellet. Tortuosity factors were higher when diffusion was assumed to occur only in the macropore ( $r > 50 \times 10^{-10}\text{m}$ ) region. In fact,  $\tau$  was unreasonably large (14 to 45) except when the pore radius for Knudsen diffusion was taken to be a constant value calculated from the macropore volume and surface area according to the equation  $2(V_g)_m/(S_g)_m$ . If diffusion is assumed to occur in all

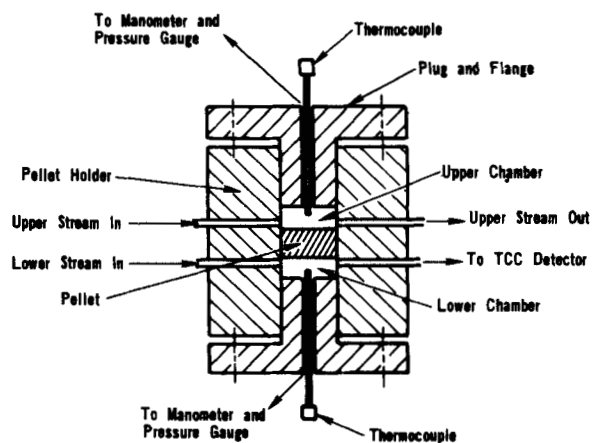


Figure 1. Schematic drawing of diffusion cell.

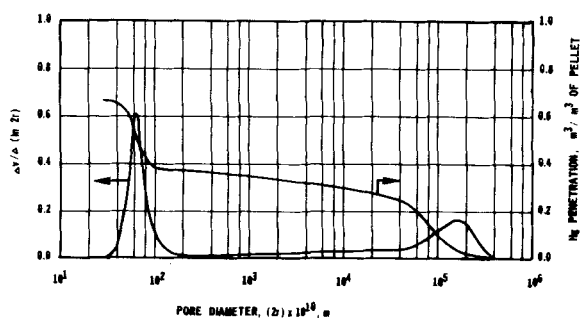


Figure 2. Cumulative volume and pore-size distribution for pellet No. 1.

the pores, the same procedure for evaluating the Knudsen contribution led to unrealistically low ( $\sim 1.0$ ) values of  $\tau$ . This is

For diffusion of gases in porous catalyst particles it is customary (Satterfield, 1970) to define a tortuosity factor  $\tau$  for a pore of radius  $r$  by the expression

$$D_e = \epsilon_p D_A(r) / \tau \quad (1)$$

The effective diffusivity  $D_e$  for component A, as evaluated from experimental data, is based upon the total pore plus solid area perpendicular to the direction of diffusion and on the most direct path (the  $x$  direction), for example, the radial coordinate for a spherical particle. The composite molecular diffusivity  $D_A(r)$  is a function of the pore radius  $r$  if Knudsen diffusion is significant. Neglecting the composition effect and at constant pressure,  $D_A$  is given (Evans, et al., 1961) for a pore of radius  $r$  by

$$\frac{1}{D_A(r)} = \frac{1}{D_{AB}} + \frac{1}{D_{KA}(r)} \quad (2)$$

where  $D_{AB}$  is the bulk diffusivity for the binary gas mixture A, B and  $D_{KA}(r)$  is the Knudsen diffusivity for A in a pore of radius  $r$ .

The advantage of the tortuosity factor as determined from Eq. 1 is that, in contrast to  $D_e$ , it is independent of the properties of the gas mixture and depends only on the catalyst pore structure. Many of these characteristics, such as a tortuous path and pore constrictions, reduce the diffusion flux causing  $\tau$  to be greater than unity, while others, for example, pore interconnections, can increase the flux.

A potential difficulty arises in using Eqs. 1 and 2 when Knudsen diffusion is important. For some monodisperse materials such as conventional silica gel, the distribution of pore sizes may be narrow so that a most probable pore radius may be used with little error to evaluate  $D_{KA}(r)$ . For a catalyst with a broad pore-size distribution, including small-diameter pores, the problem is more difficult. The conventional procedure has been to choose a single value of radius, the most probable value, to evaluate  $D_{KA}(r)$  in Eq. 2 and then  $\tau$  from Eq. 1. The results should be improved by summing the Knudsen and bulk contributions, according to Eq. 2, over the complete range of pore sizes. This concept has been used by Wakao and Smith (1972) when diffusion occurs only by the Knudsen mechanism. In the general case where both bulk and Knudsen diffusion are significant, Eq. 2 should be used for each increment of pore volume. Thus, the diffusion flux per unit of void plus nonvoid area (perpendicular to the direction of diffusion) is given by

$$N_A = \frac{-1}{\tau} \left[ \int_0^\infty D_A(r) f(r) dr \right] \frac{dC_A}{dx} \quad (3)$$

where the integration is over the entire range of pore radii. The function  $f(r)dr$  represents the void area in pores of radius between  $r$  and  $r + dr$ , per unit of total pellet area. Void-area fractions may be taken equal to void-volume fractions so that  $f(r)dr$  also represents the void volume (per unit volume of pellet), as determined

understandable since  $2V_g/S_g$ , when evaluated over the entire pore volume, underestimates the effective radius for diffusion.

The most constant and reasonable ( $\tau \approx 8$ ) values of tortuosity factor were obtained when the Knudsen and bulk contributions were summed over the total range of pore volumes. Interestingly, these  $\tau$  values did not increase appreciably for the more dense pellet. This is in contrast to observations (Kim and Smith, 1974) that  $\tau$  increases with decreases in pellet porosity, at least when the porosity changes are large. It may be that the porosity change from 0.677 to 0.569 did not result in significant changes in pore geometry. Also, generalizations about how tortuosity changes with porosity may not be reliable. For example, the extrudate-type catalyst used in our work may behave differently than  $\text{Al}_2\text{O}_3$  pellets made from spray-dried, microporous  $\text{Al}_2\text{O}_3$  particles.

from pore-size distribution data. In Equation 3, the tortuosity factor is assumed to be the same for all pores. If an average value  $\bar{D}_A$  is defined as

$$\bar{D}_A = \frac{\int_0^\infty D_A(r) f(r) dr}{\epsilon_p} \quad (4)$$

Equation 3 may be written

$$N_A = -\frac{\bar{D}_A \epsilon_p}{\tau} \frac{dC_A}{dx} \quad (5)$$

The defining equation for the effective diffusivity is

$$N_A = -D_e \frac{dC_A}{dx} \quad (6)$$

Comparison of Eqs. 5 and 6 indicates that  $D_e$  may be expressed as

$$D_e = \frac{\epsilon_p \bar{D}_A}{\tau} \quad (7)$$

Equation 7 shows that Eq. 1 is suitable for evaluating the tortuosity factor from experimental  $D_e$  values, provided that an average composite diffusivity calculated from Eq. 4 is used.

In the conventional procedure where a single, average-pore radius is employed, a question arises in choosing the proper pore radius. Usually, it has been assumed that diffusion occurs only in the macropores. Then, the Knudsen contribution is evaluated either from the most probable pore radius, a volume average value  $\bar{r}$ , determined from the macropore volume distribution, or from  $\bar{r} = 2(V_g)_m/(S_g)_m$ . While this may seem reasonable when the pellet is made by compressing microporous particles, some of the macropores (spaces between particles) may be smaller than the largest micropores. Alternately, the entire pore volume may be used to evaluate an average pore radius, either a volume average or from the equation  $\bar{r} = 2V_g/S_g$ . For a bidisperse pellet, there is usually a very small pore volume with this value of  $\bar{r}$ .

Our purpose in this study was to apply the various methods for evaluating  $\tau$  to determine the most appropriate procedure, i.e., the procedure that gave the most reasonable, and constant, values for the tortuosity factor. To do this diffusion rates and pore-volume distributions were measured for two gases,  $\text{H}_2$  and He, and for pellets, of the same unsulfided catalyst, with two different pore-volume distributions. Data were obtained at atmospheric pressure and over the temperature range 296 to 502 K.

## EXPERIMENTS

The dynamic method (Dogu and Smith, 1975) was used to determine  $D_e$ . In this method, a pulse of diffusing component in a carrier gas flows

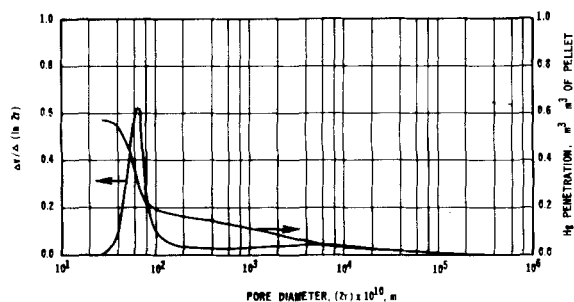


Figure 3. Cumulative volume and pore-size distribution for pellet No. 2.

TABLE 1. PROPERTIES OF CATALYST

Pellet	Compo- sition* wt. %	Surface area** m <sup>2</sup> /g	Pellet density*** $\rho_p$ , kg/m <sup>3</sup>	Total Porosity $\epsilon_p$
1	MoO <sub>3</sub>	16.2	$0.956 \times 10^3$	0.677
	CoO	5.0		
	Na <sub>2</sub> O	0.05		
2	SO <sub>4</sub>	0.3	$1.37 \times 10^3$	0.569
	Al <sub>2</sub> O <sub>3</sub>	78.45		

\* Supplied by manufacturer.

\*\* Calculated from pore-volume distribution assuming cylindrical pores. Total surface area from manufacturer, based upon N<sub>2</sub> adsorption, = 230 m<sup>2</sup>/g. Macropore surface area calculated from pore-volume distribution, ( $S_g$ )<sub>m</sub> = 11.2 m<sup>2</sup>/g.

\*\*\* The density was determined and controlled by weighing the particles before they were added to the diffusion cell (of known volume).

over the upper face of a single cylindrical catalyst pellet while pure carrier gas flows over the lower face. The pressure on the two faces is maintained at the same value to prevent convection. The concentration vs. time response curve is measured with a detector (thermal conductivity cell) located in the effluent stream from the lower face. The curved surface of the pellet is encased in a holder so that diffusion is one dimensional in the axial ( $x$ ) direction. The apparatus is the same as that described in detail by Dogu and Smith (1975) except for improvements. These changes were to minimize the volumes of the upper and lower chambers (volume =  $2.26 \times 10^{-7}$  m<sup>3</sup>) shown in the detail of the diffusion cell, Figure 3, and to minimize the dead volumes between pulse injection and upper face of the pellet and between lower face of the pellet and detector. Such changes reduced the correction necessary to obtain the first moment of the pellet itself from the observed response curve and also made the experimental arrangement more closely fit the boundary conditions used in relating the first moment  $\mu_1$  of the response curve to  $D_e$ .

The cylindrical catalyst pellets (diameter =  $9.52 \times 10^{-3}$  m, length =  $4.76 \times 10^{-3}$  m) were prepared by compressing particles ( $0.61$  to  $1.04 \times 10^{-4}$  m size range) directly in the diffusion cell. The particles were prepared by crushing and sieving a commercial, unsulfided hydrodesulfurization catalyst (HDS-20A, extrudate) from the American Cyanamid Company. Separate pellets, containing the same weight of catalyst and of the same volume, were used for diffusion and pore-size distribution measurements. Data were obtained for two pellets of widely different density. Their properties are given in Table 1 and Figures 1 and 2 show the pore-size distribution data as measured in a nominal 60,000 psi (413 MPa) mercury porosimeter.

Diffusion measurements were made on both pellets from 296 to 502 K at 1 atm pressure for two gas systems: pulses of helium in nitrogen and pulses of hydrogen in nitrogen. In each case, the input pulse ( $1.0 \times 10^{-6}$  m<sup>3</sup>) contained 2.5% He or H<sub>2</sub> in nitrogen. For this pulse composition, the concentration of diffusing component within the pellet was always very low so that using composition-independent Eq. 2 was justified. Flow rates at pellet temperature and pressure through the upper chamber (Figure 3) ranged from about  $0.5$  to  $1.0 \times 10^{-6}$  m<sup>3</sup>/s and through the lower chamber from  $0.5$  to  $5 \times 10^{-6}$  m<sup>3</sup>/s.

## RESULTS

### Dead-Volume Correction

The response curves recorded from the detector were used to calculate the observed first moments according to the equation

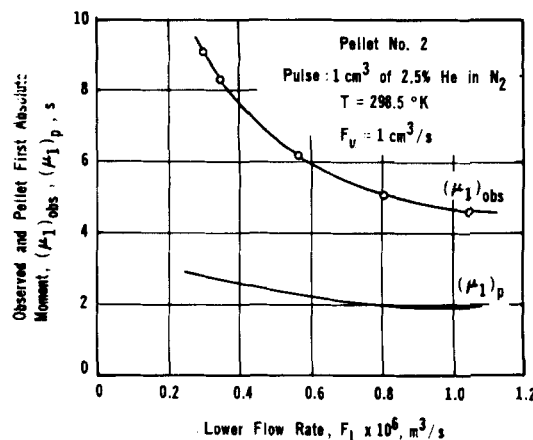


Figure 4. First absolute moment vs. lower flow rate for He-N<sub>2</sub> system at 298.5 K.

$$(\mu_1)_{\text{obs}} = \frac{\int_0^\infty R t dt}{\int_0^\infty R dt} \quad (8)$$

The expression relating  $D_e$  and the first moment  $(\mu_1)_p$  for non-adsorbing gases for the pellet is (Burghardt and Smith, 1979)

$$(\mu_1)_p = \left( \frac{\epsilon_p L^2}{6 D_e} \right) \frac{6 K_u K_L + 3(K_u + K_L) + 1}{1 + K_u + K_L} \times \frac{\theta_u(1 + K_L) + \theta_L(1 + K_u)}{1 + K_u + K_L} \quad (9)$$

where

$$K_u = A D_e / L F_u \quad (10)$$

$$K_L = A D_e / L F_L \quad (11)$$

and  $\theta_u$  and  $\theta_L$  are the mean residence times in the upper and lower chambers.

The observed first moment and  $(\mu_1)_p$  are related by the first moments of the upper stream (between injection and upper chamber inlet) and of the lower stream (between lower chamber outlet and detector, and by the first moment,  $V_s/2F_u$ , of the input pulse. This additive relation is

$$(\mu_1)_p = (\mu_1)_{\text{obs}} - \frac{V_u}{F_u} - \frac{V_L}{F_L} - \frac{V_s}{2F_u} \quad (12)$$

In order to calculate  $D_e$  from Eq. 9,  $(\mu_1)_p$  must be obtained from  $(\mu_1)_{\text{obs}}$ . This means that the dead volumes  $V_u$  and  $V_L$  are required. They cannot be evaluated with accuracy from the geometry of the system. Hence, they were determined by making two kinds of measurements of  $(\mu_1)_{\text{obs}}$  at room temperature: 1) first for different lower flow rates  $F_L$  at constant upper flow rate  $F_u$ ; and 2), then at constant  $F_L$  for various  $F_u$ . The calculational procedure may be illustrated by applying Eq. 12 at two different lower stream flow rates  $F_{L,1}$  and  $F_{L,2}$  at constant  $F_u$ . Subtracting the two resulting equations and solving for  $V_L$  gives

$$V_L = \frac{[(\mu_1)_{\text{obs},1} - (\mu_1)_{\text{obs},2}] - [(\mu_1)_{p,1} - (\mu_1)_{p,2}]}{1/F_{L,1} - 1/F_{L,2}} \quad (13)$$

Preliminary values of  $(\mu_1)_{p,1}$  and  $(\mu_2)_{p,2}$  are calculated from Eq. 9 by assuming  $D_e$  for the pellet and using known flow rates. Now a preliminary value of  $V_L$  can be obtained from Eq. 13. The data at different upper flow rates can be used in a similar way to obtain  $V_u$  using an expression analogous to Eq. 13. Finally, Eq. 12 is applied at the two  $F_L$  to calculate  $(\mu_1)_{p,1}$  and  $(\mu_1)_{p,2}$ . These results are compared with the values obtained from the assumed  $D_e$  using Eq. 9. The procedure is repeated until assumed and calculated first moments agree. The upper dead volume was  $0.746 \times 10^{-6}$  m<sup>3</sup>, independent of  $F_u$ . The lower dead volume was  $1.10 \times 10^{-6}$  m<sup>3</sup>.

TABLE 2. TORTUOSITY FACTORS BASED UPON TOTAL PORE VOLUME

Pellet	T, K	Gas Pulse/Carrier	$D_e \times 10^4$ m <sup>2</sup> /s	$D_{KA} \times 10^4$ , m <sup>2</sup> /s		$D_{AB} \times 10^4$ m <sup>2</sup> /s	$\bar{D}_A \times 10^4$ m/s			$\tau$		
				$\bar{r}^a$	$\bar{r}^b$		Eq. 4	$\bar{r}^a$	$\bar{r}^b$	Eq. 4	$\bar{r}^a$	$\bar{r}^b$
1 $\epsilon_p = 0.677$	296	He/N <sub>2</sub>	0.028	0.051	17.5	0.687	0.336	0.048 <sup>2</sup>	0.67	8.0	1.1	16.0
	365	He/N <sub>2</sub>	0.041	0.057	19.4	0.972	0.464	0.054	0.94	7.6	0.89	15.0
	411	He/N <sub>2</sub>	0.050	0.060	20.6	1.18	0.555	0.058	1.13	7.5	0.78	15.0
	455	He/N <sub>2</sub>	0.065	0.064	21.6	1.40	0.651	0.061	1.33	6.8	0.64	14.0
	498	He/N <sub>2</sub>	0.084	0.067	22.7	1.63	0.750	0.064	1.54	6.1	0.52	12.0
1	296	H <sub>2</sub> /N <sub>2</sub>	0.026	0.083	24.7	0.735	0.370	0.075	0.73	9.6	1.9	19.0
	365	H <sub>2</sub> /N <sub>2</sub>	0.042	0.092	27.4	1.05	0.516	0.085	1.03	8.4	1.4	17.0
	412	H <sub>2</sub> /N <sub>2</sub>	0.050	0.098	29.1	1.29	0.623	0.041	1.25	8.4	1.2	17.0
	457	H <sub>2</sub> /N <sub>2</sub>	0.066	0.103	30.7	1.53	0.734	0.097	1.49	7.5	0.99	15.0
	502	H <sub>2</sub> /N <sub>2</sub>	0.090	0.108	32.2	1.80	0.851	0.10	1.73	6.4	0.76	13.0
2 $\epsilon_p = 0.569$	298	He/N <sub>2</sub>	0.0094	0.035	2.18	0.694	0.138	0.033	0.53	8.4	2.0	32.0
	365	He/N <sub>2</sub>	0.0110	0.038	2.41	0.972	0.176	0.037	0.70	8.9	1.9	35.0
	411	He/N <sub>2</sub>	0.016	0.041	2.56	1.18	0.202	0.039	0.82	7.3	1.4	30.0
	456	He/N <sub>2</sub>	0.018	0.043	2.69	1.41	0.228	0.042	0.93	7.4	1.3	30.0

$$^a \bar{r} = 2V_g/S_g$$

$$^b \bar{r} = \int_0^R r dV/V_g$$

After  $V_L$  and  $V_u$  are established,  $(\mu_1)_p$  at any flow rate can be calculated from  $(\mu_1)_{obs}$  using Eq. 12. Typical results are shown in Figure 4 which is for the most dense pellet (number 2).

### Effective Diffusivities

The effective diffusivity was evaluated from  $(\mu_1)_p$  with non-linear Eq. 9 by numerical methods. A value of  $D_e$  was assumed and  $(\mu_1)_p^{calc}$  calculated for each set of upper and lower flow rates. Then the sum of the deviations between  $(\mu_1)_p$  and  $(\mu_1)_p^{calc}$  was evaluated according to the equation:

$$\phi = \sum_i [(\mu_1)_p - (\mu_1)_p^{calc}]^2 \quad (14)$$

A search technique was employed to find the minimum value of  $\phi$  and, the best value of  $D_e$ . The results for the two gas systems and the two pellets are given for each temperature in Table 2.

### Tortuosity Factors

The method proposed in this paper is to sum the diffusion flux over the entire pore volume; that is, to use Eq. 4. From Figures 1 and 2, the volume fraction  $f(r) = dV/dr$  can be evaluated. The figures give the volume  $V_g$  per unit mass of pellet, but the mass and volume of the pellet are known so that  $f(r)$  can be obtained. Then the average composite diffusivity  $\bar{D}_A$  is calculated by Eq. 4 using Eq. 2 for  $D_A(r)$ . Knowing  $\bar{D}_A$  and  $D_e$  the tortuosity factor is determined from Eq. 7. Values of  $\bar{D}_A$  and  $\tau$  obtained by this method are given in Table 2 (columns labeled Eq. 4), for He pulses in nitrogen and for N<sub>2</sub> pulses in helium for both pellets. Also given in

the table are results based upon  $D_{KA}$  determined at  $\bar{r} = 2V_g/S_g$ . In addition Table 2 includes  $D_{KA}$  and  $\tau$  values determined by calculating  $D_{KA}$  from a volume-average  $\bar{r} = \int_0^R r dV/V_g$ .

Table 3 shows the results obtained by the three methods but using only the macro-pore region ( $r > 50\text{\AA}$ ) for evaluating Knudsen and bulk diffusion. That is, it is assumed that no diffusion occurs in pores  $< 50 \times 10^{-10}\text{m}$  in radius.

### DISCUSSION

The diffusivities  $D_e$  for the two diffusing gases are nearly the same for the same pellet and for the same temperature, verifying that little adsorption occurs for N<sub>2</sub> or He. The increase in  $D_e$  with temperature is to be expected, although the magnitude is slightly greater than theory would suggest. The tortuosity factor, like  $D_e$ , is a very sensitive quantity so that the variation in  $\tau$  values between the two diffusing gases is within the limits expected from careful experimental data (e.g., p. 38, Satterfield, 1970). The diffusivity decreases significantly with decrease in pellet porosity.

Pellet 2 has considerably less macropore volume than pellet 1, as seen in Figures 1 and 2. The usual methods of determining  $\tau$ , based upon only macropores show an increase in  $\tau$  as macropore volume decreases. The results in Table 3 conform to this pattern except for those based upon  $\bar{r} = 2V_g/S_g$ . For the latter case,  $\tau$  is nearly the same for pellets 1 and 2. In Table 2 there is a significant increase in  $\tau$  for results based upon  $\bar{r}$ , but the values based upon Eq. 4 are nearly independent of pellet density.

In terms of magnitude, the results for  $\tau$  in Table 2 (using the entire pore volume) are reasonable only for the method proposed

TABLE 3. TORTUOSITY FACTORS BASED UPON MACROPORE ( $r > 50\text{\AA}$ ) VOLUME

Pellet	T, K	Gas Pulse/Carrier	$D_e \times 10^4$ m <sup>2</sup> /s	$D_{KA} \times 10^4$ , m <sup>2</sup> /s		$D_{AB} \times 10^4$ m <sup>2</sup> /s	$\bar{D}_A \times 10^4$ m <sup>2</sup> /s			$\tau$		
				$\bar{r}^a$	$\bar{r}^b$		Eq. 4	$\bar{r}^a$	$\bar{r}^b$	Eq. 4	$\bar{r}^a$	$\bar{r}^b$
1	296	He/N <sub>2</sub>	0.014	0.60	30.0	0.687	0.57	0.32	0.67	15.0	8.2	17.0
	365	He/N <sub>2</sub>	0.021	0.66	34.0	0.972	0.79	0.39	0.94	14.0	7.0	17.0
	411	He/N <sub>2</sub>	0.026	0.70	36.0	1.18	0.95	0.44	1.14	14.0	6.5	17.0
	455	He/N <sub>2</sub>	0.033	0.74	37.0	1.40	1.14	0.48	1.35	13.0	5.6	16.0
	498	He/N <sub>2</sub>	0.043	0.78	39.0	1.63	1.29	0.53	1.56	11.0	4.7	14.0
1	296	H <sub>2</sub> /N <sub>2</sub>	0.013	0.85	43.0	0.735	0.62	0.39	0.72	17.0	11.0	20.0
	365	H <sub>2</sub> /N <sub>2</sub>	0.022	0.94	47.0	1.05	0.87	0.50	1.03	15.0	8.8	18.0
	412	H <sub>2</sub> /N <sub>2</sub>	0.026	1.0	50.0	1.29	1.05	0.56	1.25	16.0	8.3	19.0
	457	H <sub>2</sub> /N <sub>2</sub>	0.034	1.0	53.0	1.53	1.25	0.62	1.49	14.0	7.0	17.0
	502	H <sub>2</sub> /N <sub>2</sub>	0.046	1.1	56.0	1.80	1.45	0.68	1.74	12.0	5.7	14.0
2	298	He/N <sub>2</sub>	0.0031	0.22	5.9	0.694	0.34	0.16	0.62	22.0	10.0	40.0
	365	He/N <sub>2</sub>	0.0039	0.24	6.6	0.974	0.44	0.19	0.85	24.0	10.0	45.0
	411	He/N <sub>2</sub>	0.0052	0.25	7.0	1.18	0.51	0.21	1.01	20.0	8.0	39.0
	456	He/N <sub>2</sub>	0.0057	0.27	7.3	1.41	0.59	0.23	1.20	20.0	7.8	41.0

$$^a \bar{r} = 2(V_g)_m/(V_g)_m$$

$$^b \bar{r} = \int_0^R r dV/(V_g)_m$$

in this paper; the values based upon  $\bar{r} = 2V_g/S_g$  are unrealistically low and those for the volume-average  $\bar{r}$  are unrealistically high. In Table 3, unrealistically high  $\tau$  result except where  $\bar{r}$  is obtained from  $2(V_g)_m/(S_g)_m$ .

It is concluded that the most reliable values of  $\tau$  are those based upon Eq. 4 using the entire pore volume (Table 2); they are of the expected order of magnitude ( $\sim 6-8$ ) and show the least variation with temperature. In principle, the tortuosity factor should be independent of temperature. However, these  $\tau$  values were evaluated using dead volumes determined from first moments measured at 296 K. Slight changes in such dead volumes with temperature could explain some of the consistent variation in  $\tau$  with temperature. It is interesting to note that these tortuosity factors do not increase with decrease in porosity (pellet 1 to pellet 2). This may be due to the relatively small change in  $\epsilon_p$  (from 0.677 to 0.569). For large reductions in porosity a significant increase in tortuosity would be expected, for example, as observed by Kim and Smith (1974) where porosity was reduced by sintering NiO particles. Perhaps there was not a significant difference in arrangement of the particles in our two pellets.

It is also interesting that the tortuosity factors based upon diffusion only in the macropores (Table 3) and with  $\bar{r} = 2(V_g)_m/(S_g)_m$  are about the same as the preferred results in Table 2. We can find no justification for this arrangement since  $\bar{r} = 2V_g/S_g$  is derived by assuming a parallel pore model with all pores (cylindrical) of the same radius.

#### ACKNOWLEDGMENT

Financial support for this research was provided by a Fellowship from the Peoples Republic of China and by NSF Grant CPE 8026101. Phillips Petroleum Company provided the catalyst.

#### NOTATION

$A$	= cross-sectional area of cylindrical pellet, $m^2$
$C_A$	= concentration of diffusing component A, $m^2/s$
$D_A(\tau)$	= composite diffusivity of A, $m^2/s$ ; $\bar{D}_A$ is the average value defined by Eq. 4
$D_{AB}$	= bulk molecular diffusivity of binary gas mixture, AB, $m^2/s$
$D_{KA}(\tau)$	= Knudsen diffusivity of A, $m^2/s$
$D_e$	= effective diffusivity of A in catalyst pellet, defined by Eq. 6
$F_u$	= flow rate through upper chamber, $m^3/s$
$F_L$	= flow rate through lower chamber, $m^3/s$
$f(r)$	= pore-size distribution function; $f(r)dr$ is the pore area

$K_u, K_L$	= parameters defined by Eqs. 10 and 11
$L$	= pellet length, m
$N_A$	= diffusion rate of A per unit of void plus nonvoid area, $mol/(m^2)(s)$
$R$	= response reading (proportional to concentration)
$S_g$	= pore surface area per unit mass of pellet, $m^2/kg$
$r$	= radius of cylindrical pore, m
$t$	= time, s
$V$	= pore volume per unit volume of pellet
$V_g$	= pore volume per unit mass of pellet, $m^3/kg$
$V_L$	= dead volume in lower flow stream, $m^3$
$V_s$	= volume of injection pulse, $m^3$
$V_u$	= dead volume in upper flow stream, $m^3$
$x$	= length of most direct diffusion path, m

#### Greek Letters

$\epsilon_p$	= total porosity of catalyst pellet
$\tau$	= tortuosity factor for catalyst pellet
$(\mu_1)_p$	= first absolute moment for diffusion through catalyst pellet, corrected for dead volumes, s
$(\mu_1)_{obs}$	= observed first moment between injection located and detector, s
$\theta_L, \theta_u$	= mean residence times, $V_L/F_L, V_u/F_u$ , in the lower and upper
$\phi$	= sum of deviations defined by Eq. 14

#### Subscripts

1,2	= flow rates 1 and 2
m	= macropores

#### LITERATURE CITED

- Dogu, G., and J. M. Smith, "A Dynamic Method for Catalyst Diffusivities," *AIChE J.*, **21**, 58 (1975).
- Evans, III, R. B., G. M. Watson, and E. A. Mason, "Gaseous Diffusion in Porous Media at Constant Pressure," *J. Chem. Phys.*, **35**, 2076 (1961).
- Kim, K. K., and J. M. Smith, "Diffusion in Nickel Oxide Pellets, Effects of Sintering and Reduction," *AIChE J.*, **20**, 670 (1974).
- Satterfield, C. N., "Mass Transfer in Heterogeneous Catalysis," p. 33, M.I.T. Press, Cambridge, MA (1970).
- Wakao, N., and J. M. Smith, "Diffusion in Catalyst Pellets," *Chem. Eng. Sci.*, **17**, 825 (1962).

Manuscript received November 9, 1981; revision received February 8, and accepted March 4, 1982.